ENERGY LOSS SPECTRA OF ELECTRONS COLLIDING WITH INERT GAS ATOMS

V. V. AFROSIMOV, Yu. S. GORDEEV, V. M. LAVROV, and S. G. SHCHEMELININ

A. F. Ioffe Physico-technical Institute, Academy of Sciences, U.S.S.R.

Submitted January 31, 1968

Zh. Eksp. Teor. Fiz. 55, 1569–1577 (November, 1968)

The interaction of 3- and 4-keV electrons with electron shells of Ne, Ar, Kr, and Xe atoms was studied. An electron beam was passed through a chamber filled with one of the gases, and the energies of electrons scattered at fixed angles were determined with an electrostatic analyzer. The inelastic energy loss spectra of electrons for several scattering angles and the angular dependences of the scattering cross sections for several values of the inelastic losses were obtained (for energy losses between 0 and 450 eV, and scattering angles from 1° to 12°. The inelastic energy loss spectra of electrons interacting with the outer shells of the different atoms are similar and possess a complex structure characterized by two maxima. One maximum is located at energies only slightly above the ionization threshold. The location of the second maximum depends on the scattering angle and approximately satisfies the conditions for which the momentum lost by a fast electron is transferred completely to an electron expelled from the atom. The inelastic energy loss spectra for electrons interacting with inner shells are dissimilar for the different atoms. The loss spectrum for the N shell of the xenon atom is compared with theoretical calculations based on the single-particle approximation with account taken of many-particle effects. It is found that in this case many-particle effects play an important role.

INTRODUCTION

ATOMIC energy levels are now being investigated successfully by analyzing the inelastic energy loss spectra of fast electrons scattered by atoms. The energy resolution attained by this technique[1] can exceed the resolution of optical methods based on the investigation of photoabsorption. The method of electron energy loss analysis possesses the merit of convenient and simple application to a broad range of the energy losses, from a few eV to many hundreds of eV. It is very difficult to prepare sources of electromagnetic radiation having a continuous spectrum in the same region of quantum energies.

The analysis of inelastic electron energy losses has been used until very recently to investigate mainly interactions between electrons and outer shells of atoms. Inelastic electron scattering with large energy transfer in interactions between electrons and inner shells has been studied only for solid films and in a narrow range of small scattering angles.[2,3] Only very recently have reports been published about investigations of inelastic electron scattering in single collisions with gas atoms accompanied by the excitation and ionization of inner atomic shells.[4,5]

The investigation of energy loss spectra over a broad range is of interest because it provides information about the energies and probabilities of inelastic transitions for both outer and inner atomic shells.

In the present work, which is a continuation of[4], we have investigated the energy loss spectra associated with interactions between fast electrons and different shells of Ne, Ar, Kr, and Xe atoms. The initial electron energies were 3 and 4 keV, the energy losses lay in the interval from 0 to 450 eV, for electron scattering angles from 1° to 12°.

EXPERIMENT

Figure 1 shows the experimental arrangement for analyzing inelastic electron scattering. A collimated electron beam enters the collision chamber K containing the test gas. Electrons scattered at an angle ϑ and traversing the collimator S_3–S_4 undergo energy analysis in parallel-plate electrostatic analyzer A. Following the analyzer the electrons impinge on an electron
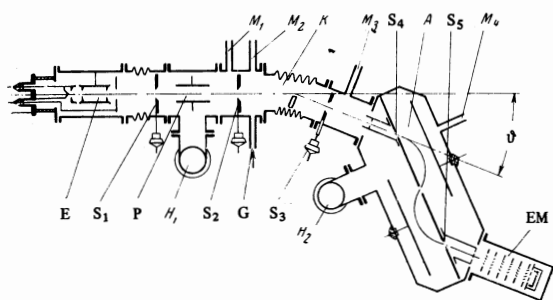
FIG. 1. Scheme of experimental apparatus used to investigate inelastic electron scattering in gases. E — electron gun, $S_1 - S_4$ — collimating slits, P — plates deflecting electron beam, K — collision chamber, A — electrostatic analyzer, of electron energies, 0 — rotation axis of scattered electron collimator $S_3 - S_4$ and energy analyzer, EM — electron multiplier, $M_1 - M_4$ — tubes of ion gauges, G — gas inlet tube, H_1 and H_2 — high vacuum pumps.

multiplier EM whose output current is amplified by an electrometer before being fed to a recording potentiometer, wherein the moving trace-recording tape is synchronized with changes in the voltage applied to the analyzer plates. The energy loss (R) spectrum is thus registered continuously. By rotating the collimator and analyzer about an axis passing through the collision chamber we also obtain the angular distributions of scattered electrons exhibiting a fixed energy loss. Our apparatus permitted 30' angular resolution and an energy resolution of 1250. All the measurements were obtained under conditions that provided for single collisions between fast electrons and gas atoms.

Our apparatus thus enabled us to determine directly the differential cross sections $\partial^2\sigma/\partial R\partial\omega$ for electron scattering per unit solid angle and per unit interval of inelastic energy loss, for different fixed values of the energy loss R and scattering angle ϑ. The automatic registration of the loss spectrum for given electron scattering angles yielded the dependence of the differential cross sections on the inelastic loss. To investigate the spectra of inelastic energy losses, which was the principal aim of the present work, it was sufficient to obtain relative measurements of the differential cross sections. Therefore the accuracy of the measurements depends on the possible distortions of the spectra.

The distortions of the automatically registered loss spectra are caused mainly by the drift of the parameters affecting the signal from the registering system while in operation. These parameters include the gas pressure in the chamber, the initial electron beam current, and the amplification of the electron multiplier. Under our experimental conditions the drift of these parameters remained practically constant during the time required for registering a spectrum. Therefore the drift-induced spectral distortions at the given tape speed depended only on the energy interval ΔR between the points of the spectrum. A few errors in determining the shapes of the spectra also resulted from noise of the secondary multiplier and the electrometric amplifier.

The spectra distortions can be represented quantitatively by the accuracy achieved in determining the ratio $\sigma(R + \Delta R)/\sigma(R)$ of cross sections at different spectral points. Under our conditions the error of this ratio was

$$\delta[\sigma(R + \Delta R) / \sigma(R)] = (0.05\Delta R + n) \%,\qquad(1)$$

where ΔR is the energy interval (eV) between the compared points, and n is the noise level, which depended on the magnitudes of the cross sections and comprised 10% for cross sections of the order 10^{-20} cm^2/eV-sr. The error of the inelastic loss measurements was $\pm(0.01R + 1.5\text{ eV})$.

It should be noted that calibration of our apparatus enabled us to convert the relative cross sections to absolute units. Absolute measurements of the differential scattering cross sections are unavailable for our electron energy range (1—7.5 keV). We therefore used as our calibration standard the measured cross sections for the elastic scattering of 25-keV electrons in Ar.[6] These experimental cross sections were converted to the 7.5-keV initial electron energy and were used to normalize the measurements obtained with our apparatus at this energy. The conversion to a different energy was performed in the first Born approximation, according to which the cross section would depend only on the product $\sqrt{T_0}\sin\vartheta$, where T_0 is the initial electron energy.

As an additional check we compared our derived standard cross sections with those calculated theoretically by Mott and Massey[7] for the elastic scattering of 7.5-keV electrons by Ar atoms. The calculations in[7] were performed in the first Born approximation using the Hartree and Thomas-Fermi approximations for the atomic factor, and yielded cross sections that differed from the experimental standards by at most 10% for scattering angles $\vartheta \geq 3°$. Therefore the approximations used in the calculations are quite reliable in this range.

RESULTS AND DISCUSSION

Figure 2 shows the energy loss spectra of electrons scattered by Ne, Ar, Kr, and Xe atoms. In addition to the elastic scattering peak at R = 0 (the shape of which is characteristic for the overall resolution of the apparatus), we observe peaks corresponding to interactions of the fast electrons with different electron shells of the atoms. For Ne we investigated only the interaction with the outer shell. The spectra for Ar, Kr, and Xe reveal clearly the distinct regions corresponding to electron interaction with the outer and inner shells. These regions are identified by comparing the starting point of each peak with the ionization potential of the corresponding shell.

The spectral regions representing the electron interactions with outer shells are similar for all four inert gases and exhibit certain common characteristics. At the angles shown in Fig. 2 the considered spectral regions are associated mainly with the ionization of the outer shells. The contribution from the excitation of discrete levels is observed distinctly at the scattering angles 1° and 2° in the case of Ne. For the other targets these processes begin to play an important role at even smaller scattering angles than those shown in the figure.

We shall now consider in greater detail the spectra of losses in outer shells, taking argon as an example. The loss spectra for electrons scattered at 1.5—12°
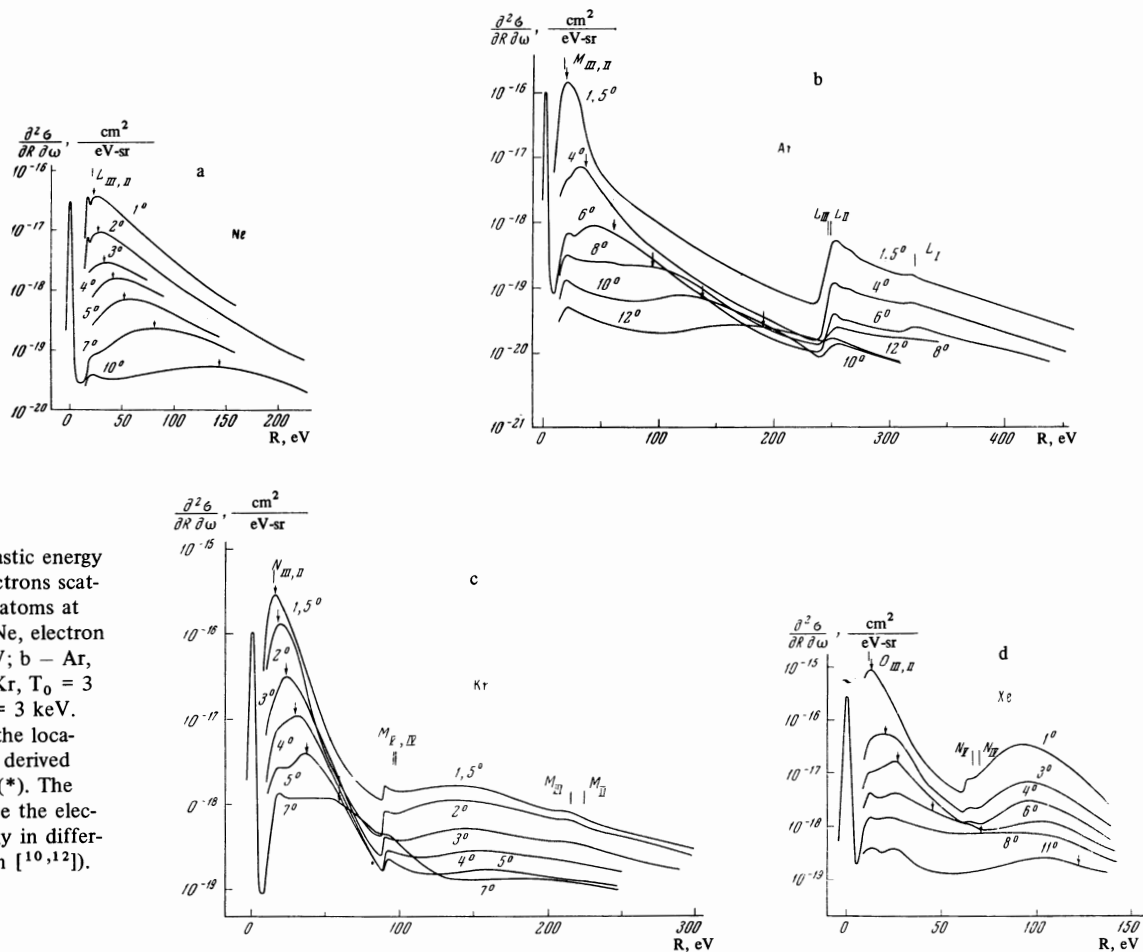
FIG. 2. Inelastic energy loss spectra of electrons scattered by inert gas atoms at fixed angles. a — Ne, electron energy $T_0 = 4$ keV; b — Ar, $T_0 = 4$ keV; c — Kr, $T_0 = 3$ keV; d — Xe, $T_0 = 3$ keV. Arrows designate the locations of the peaks derived from the relation (*). The vertical bars denote the electron binding energy in different subshells (from [10,12]).

from Ar atoms (Fig. 2b) exhibit a steep rise of the cross section beginning at the ionization threshold. At about 3 eV above the threshold the inelastic scattering cross section reaches a maximum that remains practically constant at this energy for the different scattering angles. At angles $\vartheta \geq 6°$ this near-threshold maximum is accompanied by a second maximum, the location of which varies with the angle. As the scattering angle increases the maximum is shifted toward higher losses; its width increases, while its height falls below that of the near-threshold maximum. The second maximum vanishes at $\vartheta = 8°$, but reappears at 10° and 12°. The presence of only a single maximum at scattering angles below 6° may be an indication that at such angles the second maximum is merged with the near-threshold maximum.

The fact that the location of the second maximum depends on the scattering angle suggests that this maximum depends on the conditions of momentum transfer to the electron that is ejected from the atom. We know[8] that the maximum cross section for inelastic electron-atom scattering can occur when the transferred momentum equals the momentum of the ejected electron. The location of this maximum in the energy loss spectrum will be obtained approximately from the relation

$$R_{max} = u_i + \vartheta^2 T_0,   (*)$$

where u_i is the ionization potential.

The arrows in Fig. 2 indicate the locations of maxima that have been calculated by means of the relation (*). The agreement with experiment is satisfactory; better agreement is observed at larger angles (10° and 12°) than at $\vartheta < 8°$.

It is of interest that a dependence similar to (*) of the cross-sectional maximum on the scattering angle can be associated with processes of a different nature. This kind of dependence has been observed in the scattering of electrons on solid films, accompanied by the excitation of plasma oscillations.[9]

The spectra of energy losses in the outer shells of Ne (Fig. 2a) and Kr (Fig. 2c) resemble the Ar spectum. Some differences appear in the Xe spectra (Fig. 2d). A second maximum, located in accordance with its dependence on the scattering angle, is observed in the Xe spectra only for energy losses up to about 27 eV. This location is found for the maximum at 4°, with no shift at larger angles, although the height of the maximum decreases rapidly. For losses above 27 eV the Xe spectra contain no maximum of this type. However the spectral regions of Xe that correspond to (*) at $R > 27$ eV exhibit a slower decrease of the cross section as the loss increases than in the adjoining regions. This effect appears to explain the absence of a cross sectional minimum in the region of transition from ionization of the outer Xe shell to ionization of an inner shell at $\vartheta = 8°$.

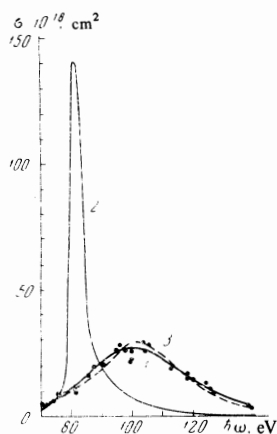Unlike the energy loss spectra for the outer shells,

FIG. 3. Energy dependence of the photoabsorption cross section for the N shell of xenon. 1 — results of present work, converted to the photoabsorption cross section in the dipole approximation; 2 — photoabsorption cross section calculated in the single-particle approximation[15]; 3 — photoabsorption cross section calculated with account of many-particle effects.[16,17] Experimental points were taken from[14].

the spectra for the inner shells of Ar, Kr, and Xe exhibit significant differences. The loss spectrum for the L shell of Ar has a pronounced "hydrogen-like" asymmetric form. It is characterized by a sharp rise of the cross section from the L-shell ionization threshold (~245 eV) and a relatively slow decline from the maximum. Two peaks are observed in the L-shell spectra of Ar. The peak at 265 eV is evidently associated with the simultaneous excitation or ionization of the M and L shells. The second peak represents ionization of the L_I subshell. The location of the latter peak agrees well with the binding energy of L_I electrons (about 320 eV, according to the most recent data[10,11]). The spectrum for the M shell of Kr and even more especially the spectrum for the N shell of Xe are more symmetric and have a flatter left-hand slope than the spectrum for L-shell ionization of Ar.

The maxima of these spectra are shifted far above the ionization thresholds of the respective shells: 50—60 eV above for Kr and 30—40 eV above for Xe. With increase of the scattering angle the maximum are shifted slightly toward still higher losses.

The prominences at 90 eV for Kr and 65 eV for Xe appear to represent unresolved discrete lines corresponding to the excitation of the M shell in Kr and the N shell in Xe. An exact interpretation is difficult because the literature[10,12] contains widely divergent values of the inner electron binding energies.

A comparison between our energy loss spectra for Kr and Xe at different scattering angles and calculations of the same spectra in the single-particle approximation using Herman-Skillman wave functions[13] revealed considerable quantitative discrepancies between our experiment and the theory, especially in the case of Xe. A similar divergence between experiment[14] and calculations[15] had previously been observed in the region of N-shell ionization when photoabsorption by Xe was investigated.

In Figure 3 experimental and calculated results are compared for the photoabsorption cross section of the xenon N shell. The calculation in the single-particle approximation (curve 2) had been performed by Cooper;[15] calculations involving many-particle effects (curve 3) had been performed by Brandt et al.[16] and by Amusia et al.[17] The experimental curve 1 was obtained by converting our measurements to photoabsorption cross sections, in the dipole approximation.

The separate experimental points represent the photoabsorption cross sections measured by Lukirskiĭ et al. and by Ederer.[14]

Figure 3 shows that our data agree well with the experimental photoabsorption cross sections. The calculation in the single-particle approximation yields results that differ greatly from the experimental results with respect to both the position of the maximum and the spectral shape. These discrepancies are eliminated almost completely by the calculation of many-particle effects.

The analysis of the energy loss spectra also leads to definite conclusions regarding the kinetic energy distribution of electrons ejected from the different atomic shells. In a study that allows for inelastic interactions between the incoming electron and several atomic electrons it may be assumed that the energy lost by the incident electron is expended in removing one electron and in transferring kinetic energy to the latter. Therefore the portion of the energy loss spectrum from the ionization threshold to the region of interaction between the incident electron and an inner shell can be regarded as the energy spectrum of electrons ejected from the outer shell by electrons scattered at an angle ϑ. Integration over all scattering angles gives the total energy spectrum of electrons ejected from the outer shell. When the lost energy exceeds the ionization potential of the inner shell, the spectrum of electrons ejected from the inner shell is imposed on the spectrum of electrons ejected from the outer shell. For example, the segment of the argon loss spectrum (Fig. 2b) from the first ionization potential at 15.7 eV to ~245 eV represents the energy spectrum of electrons ejected from the M shell. The separation between the ionization threshold and the maximum gives the most probable kinetic energy of the ejected electrons. It follows from Fig. 2b that this energy is ~3 eV in the case of the M shell of Ar. An examination of the loss spectra (Fig. 2b) in the region of L-shell ionization ($R \geq 245$ eV) shows that the most probable kinetic energy of electrons ejected from the $L_{II,III}$ subshell is 5—7 eV. This energy is evidently governed by the fact that electrons leaving the $L_{II,III}$ subshell must surmount the centrifugal potential barrier. Despite the large difference between the ionization potentials of the M and L shells there is no appreciable difference between the most probable electron energies of electrons ejected from these two shells.

In addition to the energy spectra, we investigated the angular distributions, i.e., the dependence of the differential cross section on the scattering angle at different fixed values of the energy loss. Figure 4 shows an example of the angular distributions obtained for scattering by Ar atoms. The angular distributions have a common characteristic: the more the energy loss exceeds the ionization threshold of a given shell, the less steeply the angular distribution falls off as ϑ increases. Curves 1 and 4 show that so long as only the outer shell is involved in the interaction the increase of the energy loss results in less steepness of the angular distributions. When we go from curve 4 to curve 5 we make a transition to L-shell ionization, which manifests itself in an appreciable enhancement
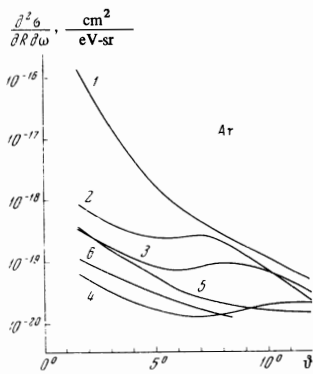
FIG. 4. Differential cross sections for inelastic electron scattering from Ar atoms versus scattering angles for several values of the inelastic energy loss R: 1 — 20, 2 — 100, 3 — 140, 4 — 220, 5 — 260, and 6 — 340 eV. Initial electron energy T_0 = 4 keV.

the steepness in the angular distribution. With further increase of the energy loss (curve 6) the angular distributions again become increasingly flatter.

Figure 4 shows that some of the angular distributions possess a maximum which shifts towards larger angles as the energy loss increases. This maximum is of the same character as the second maximum in the loss spectra (Fig. 2) corresponding to the relation (*).

[1] J. Geiger and B. Schröder, in Abstracts of Papers, Fifth Intern. Conf. on the Physics of Electronic and Atomic Collisions, Leningrad, Nauka, 1967, p. 563.

[2] G. Ruthemann, Naturwiss. 29, 648 (1941); Ann Physik 2, 113 and 135 (1948).

[3] J. Hillier, Phys. Rev. 64, 318 (1943); J. Appl. Phys. 15, 663 (1944).

[4] V. V. Afrosimov, Yu. S. Gordeev, V. M. Lavrov, and S. G. Shchemelinin, in Abstracts of Papers, Fifth Intern. Conf. on the Physics of Electronic and Atomic Collisions, Leningrad, Nauka, 1967, p. 127.

[5] M. J. Boness, G. D. Hale, J. B. Hasted, and I. Larkin, in Abstracts of Papers, Fifth Intern. Conf. on the Physics of Electronic and Atomic Collisions, Leningrad, Nauka, 1967, p. 577.

[6] J. Geiger, Z. Physik 177, 138 (1964).

[7] N. F. Mott and H. S. W. Massey, Theory of Atomic Collisions, 2nd ed. Oxford Univ. Press, 1949 (Russ. transl., IIL, (1951).

[8] H. A. Bethe, Quantenmechanik der Ein- und Zwei-Elektronenprobleme, Handbuch der Physik XXIV/1, Julius Springer, Belin, 1933 (Russ. transl., ONTI, 1935).

[9] H. Watanabe, J. Phys. Soc. Japan 11, 1112 (1956).

[10] J. A. Bearden and A. F. Burr, Rev. Mod. Phys. 39, 125 (1967).

[11] W. Mehlhorn, Z. Physik 208, 1 (1967).

[12] K. Codling and R. P. Madden, Phys. Rev. Lett. 12, 106 (1964).

[13] M. Ya. Amusia, N. A. Cherepkov, and S. I. Sheftel, in Abstracts of Papers, Fifth Internal Conf. on the Physics of Electronic and Atomic Collisions, Leningrad, Nauka, 1967, p. 130.

[14] A. P. Lukirskiĭ, I. A. Brytov, and T. M. Zimkina, Opt. Spektrosk. 17, 438 (1964) [Opt. Spectrosc. 17, 234 (1964)]; D. L. Ederer, Phys. Rev. Lett. 13, 760 (1964).

[15] J. W. Cooper, Phys. Rev. Lett. 13, 762 (1964).

[16] W. Brandt, L. Eder, and S. Lundqvist, J. Quantitative Spectroscopy and Radiative Transfer 7, 185 (1967).

[17] M. Ya. Amusia, N. A. Cherepkov, and S. I. Sheftel, Phys. Lett. 24A, 541 (1967).

Translated by I. Emin
174